Dirty displacive ferroelectrics*†

Gerald Burns
IBM Thomas J. Watson Research Center, Yorktown Heights, New York 10598
(Received 28 July 1975)

We define a dirty displacive ferroelectric material as a displacive ferroelectric in which each unit cell is different from every other unit cell yet there is an average translational symmetry. The experimental results of the temperature dependence of the optic index of refraction $n(T)$ in two dirty displacive ferroelectrics with the tungsten-bronze crystal structure are presented. In this one crystal system these data show that as the amount of disorder increases the behavior of $n(T)$ becomes *qualitively* different from what is expected in normal ferroelectrics. We argue that this phenomenon is related to the following observation which we have previously reported: In *all* displacive ferroelectrics, in the ferroelectric phase, the Lyddane-Sachs-Teller (LST) relationship does not correctly predict the temperature dependence of the clamped low-frequency dielectric constant $\epsilon(0)$. A more complete derivation of a simple model that explains this result is given. This model considers the mechanism by which localized impurities or deviations from stoichiometry are coupled to the optic modes and shows that this type of impurity contribution to $\epsilon(0)$ can be considerably enhanced by this coupling. Thus, in $BaTiO_3$ an impurity concentration of as little as 3×10^{17} cm^{-3} can explain the very large disagreement (a factor 5) in the ratio of the value of $\epsilon(0)$ measured by standard and capacitance techniques to the LST calculations of $\epsilon(0)$. In dirty displacive ferroelectrics there is no recognizable soft optic vibrational mode. Thus, to describe the existence of large peaks in $\epsilon(0)$ and the qualitatively unexpected behavior in $n(T)$ we extend the ideas of the model, used to explain the $BaTiO_3$ data, to encompass a distribution of localized charges. The contribution to $\epsilon(0)$ from one frequency range of a localized impurity oscillator can be enhanced by not only the optic modes but also by those impurities which have a higher frequency of oscillation. Since in dirty displacive ferroelectrics one has essentially 10^{23} cm^{-3} impurities, such effects can be very important. Further, localized regions with very high dielectric constant will tend to polarize statically or dynamically far above the transition temperature T_c. These localized regions of polarization can explain the $n(T)$ data. In fact one may invert the process and, using these data, obtain a temperature-dependent polarization $P(T)$, or more exactly, $|P(T)|$. This $P(T)$, which involves no adjustable parameters, compares well with the reversable spontaneous polarization P_s in the ferroelectric phase. We believe that this model, which does not necessarily involve a soft optic mode, explains the behavior of dirty displacive ferroelectrics.

I. INTRODUCTION

The connection between lattice dynamics and ferroelectricity has been emphasized by Cochran.[1] The connection is via the $3n-3$ optic modes at small wave number ($k\approx0$) (n equals the number of atoms in a primitive cell). The class of ferroelectrics that Cochran has treated is displacive ferroelectrics. The latter are defined as materials in which the atomic positions at a temperature just below the ferroelectric transition temperature T_c can be considered as resulting from small displacements from the positions in the nonferroelectric phase.[2] In order-disorder ferroelectrics,[2] in contrast to displacive ferroelectrics, there is a double well representing energy vs displacement, and the separation between the two minima in the double well is of the order of the internuclear distance.

In the high-temperature phase, $T>T_c$, the clamped dielectric constant $\epsilon(0)$ usually exhibits a Curie-Weiss law,

$$\epsilon(0)=C/(T_c-T), \tag{1}$$

where C is the Curie constant and the measurement is along the axis that for $T<T_c$ is a polar axis. An important aspect of the connection with lattice dynamics is via the Lyddane-Sachs-Teller (LST) relation[1,2]

$$\frac{\epsilon(0)}{\epsilon_\infty}=\prod_i\frac{\omega_{\mathrm{LO}i}^2}{\omega_{\mathrm{TO}i}^2}=\frac{\omega_{\mathrm{LO1}}^2\omega_{\mathrm{LO2}}^2\cdots}{\omega_{\mathrm{TO1}}^2\omega_{\mathrm{TO2}}^2\cdots}, \tag{2}$$

where ϵ_∞ is the square of the optic index of refraction and the product is over all the longitudinal optic (ω_{LO}) and transverse optic (ω_{TO}) modes. If the lowest transverse optic mode, ω_{TO1}, is the most temperature dependent it is called the "soft mode," and Eq. 2 immediately results in Eq. 3(a) to describe the dependence on $\epsilon(0)$. If the Curie-Weiss law is obeyed, then the result is Eq. 3(b):

$$\omega_{\mathrm{TO1}}^2=A'/\epsilon(0), \tag{3a}$$

$$\omega_{\mathrm{TO1}}^2=A(T_c-T). \tag{3b}$$

Experimental verification of the temperature dependence of a soft optic mode, as predicted from Eqs. (3), was first found in $SrTiO_3$ by infrared[3] and neutron diffraction[4] and then in $KTaO_3$, also by infrared[5] and neutron diffraction.[6] These early results, along with infrared measurements of several materials at one temperature,[7] have been

taken as a verification of Cochran's idea. However, care must be taken in drawing general conclusions from these results, since neither $SiTiO_3$ nor $KTaO_3$ is a ferroelectric although both have large temperature-dependent dielectric constants. Early temperature-dependent work in $BaTiO_3$ is less clear.[8]

We have pointed out[9] that for measurements in the ferroelectric phase, the LST relation does not correctly predict $\epsilon(0)$. This statement applies to all the materials for which reliable data are known for the TO and LO modes as well as the clamped dielectric constant. Further, in $BaTiO_3$, the temperature dependence predicted by the LST relation is very different from what is measured, and most of the contribution to $\epsilon(0)$ comes not from the lowest mode but from the next higher-lying mode.[10] In order to make these points more clearly, we define two terms. Let ϵ_m be the value of the clamped dielectric constant obtained from the LST relation, Eq. (2). Thus, ϵ_m is the dielectric constant predicted by the lattice modes. Let ϵ_{cap} be the experimentally measured clamped dielectric constant, as measured by capacitance techniques. Naturally, both ϵ_{cap} and ϵ_m vary with temperature. We have pointed out[9] that in the ferroelectric phase $\epsilon_{cap}/\epsilon_m > 1$, and this ratio gets larger as T approaches T_c from below. For example, in $BaTiO_3$, an archetypal displacive ferroelectric, $\epsilon_{cap}/\epsilon_m = 2.4$ at room temperature and 5.0 at 100 °C, where $T_c = 135$ °C. Thus, the temperature variation of $\epsilon_{cap}/\epsilon_m$ is very large. A possible explanation for this has been given[11] and will be further explored in this paper. The explanation involves the coupling of the soft mode to impurities or any charged defects that have relatively low frequencies, $\sim 1 - 10$ cm^{-1}. The contribution to the clamped dielectric constant from these charged defects can be considerably enhanced (by a factor $>10^2$) when coupled to a soft mode. If this explanation can be shown to be physically justified, than the soft-mode ideas are qualitatively correct but just need some minor corrections to explain $\epsilon(0)$ quantitatively in the ferroelectric.

We have also pointed out that there is a class of apparently displacive ferroelectrics that show a temperature variation of the optic index of refraction that is in *qualitative* disagreement with what is expected in ferroelectric materials.[12] We have called these materials "dirty displacive ferfoelectrics," and this term is defined as a crystal in which each unit cell is different from every other unit cell yet possesses an average translational symmetry. For example, the crystal $Pb(Mg_{1/3}Nb_{2/3})O_3$ has the ABO_3 perovskite crystal structure (high-temperature space group O_h^1-$Pm3m$) and, in principle, the B-site ions could be ordered[13] with two (111) planes containing only Nb ions and the next (111) plane containing Mg ions. In fact the B-site ions are not ordered, but the site is randomly occupied and thus the crystal is a dirty displacive ferroelectric.

There is a good deal of work, principally in Russia,[14] on many mixed systems and other perovskite materials that are called ferroelectrics with a diffuse phase transition. This means that the dielectric peak as a function of temperature is not sharp. Although some of these materials are undoubtedly dirty displacive ferroelectrics, others appear to be normal compounds with full translational symmetry. The diffused phase transition has been interpreted[14] as due to macroscopic composition variations, i.e., different macroscopic regions of the crystal have different compositions and thus different T_c's. We believe that macroscopic composition variations are not important in the materials discussed here, while local (one unit cell to the next) variations are of paramount importance.

In this paper we present experimental data of the temperature dependence of the index of refraction, $n(T)$, for several ferroelectric crystals with the tungsten-bronze crystal structure[2] (high-temperature space group D_{4h}^5-$P4/mbm$). For the particular crystals discussed here the chemical formula, referred to the high-temperature unit cell, is $K_{2-2x}^+ Sr_{1+x}^{2+}(NbO_3)_{10}$. The stoichiometric formula has $x = 0$ or $K_2Sr_4(NbO_3)_{10}$. As will be discussed in the experimental section, for $x = 0$ it is possible for the crystal to have each unit cell the same as every other one. However, for $x > 0$ this is not possible in general. Thus, in principle, as x is varied one can vary the amount of disorder in the crystal. This could not be done in the earlier work[12] where $n(T)$ of several different crystal systems was measured but in no *one* system could the amount of disorder be varied. The experimental results for $n(T)$ clearly show that as the crystal system becomes more disordered, $n(T)$ becomes qualitatively different from the expected ferroelectric behavior. Thus, the results in the disordered tungsten-bronze material are in excellent agreement with the earlier work.

We should point out that the fact that $\epsilon_{cap}/\epsilon_m > 1$ for displacive ferroelectrics, where one considers the $3n - 3$ optic modes contributing to ϵ_m, is distinctly different from similar considerations in ferroelectric materials that have order-disorder transitions. In order-disorder materials the major contribution to $\epsilon(0)$ does not come from the optic modes but from some low-frequency motion that typically[15] has a temperature-dependent Debye-type relaxation frequency less than 1 cm^{-1}. For example, in $NaNO_2$ the important ferroelectric

motion is movement of the NO_2^- group where the group moves a fixed entity with the dipole moment pointing either parallel or antiparallel to the spontaneous polarization direction. Motion from one such position to the other is not an optic mode but is a low-frequency Debye relaxation mode.[16] Independent of this Debye relaxation mode, $NaNO_2$ has $3n-3$ (=9) optic modes. These modes have been studied by Raman[17,18] and infrared techniques.[19,20] They contribute only a very small amount to $\epsilon(0)$ along the ferroelectric axis, although an attempt to correlate the frequencies and linewidths of certain optic modes to $\epsilon(0)$ has been made.[18]

II. EXPERIMENTAL

In 1958, Francombe and Lewis[21] recognized that the structure of $PbNb_2O_6$ was similar to that of certain metal-like materials known as tungsten-bronzes. In 1967 it was discovered that a large number of alkali alkaline earths have this crystal structure and are ferroelectric.[22,23] These have the general formula $A_2^+B_4^{2+}(NbO_3)_{10}$, with one of these formula units per tetragonal unit cell. Figure 1 shows a tetragonal unit cell observed along the ferroelectric c axis. The structure can be thought of as corner-linked NbO_6 octahedra.[2,21] In the perovskite structure the octahedra are connected so that fourfold cavities are left for other atoms. However, in the tungsten-bronze structure the octahedra are connected so that fourfold- as well as fivefold- and threefold-like cavities result. These are shown in Fig. 1 and labeled α, β, and γ sites, respectively.

It has been argued[22,23] that in materials with the formula $A_2B_4Nb_{10}O_{30}$ the four B ions will tend to order on the four β sites and the two A ions will tend to order on the two α sites. The γ sites are considerably smaller then the α or β sites, and

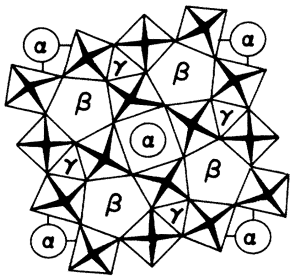

FIG. 1. Projection, looking down the ferroelectric c axis, of a tetragonal tungsten-bronze structure. The dark crosses represent NbO_6 octahedra with Nb ions at the centers and O ions at the corners of the octahedra. The α, β, and γ sites are situated in a plane $c/2$ above the Nb ions. The unit cell, as shown here, is one octahedron high.

apparently only very small ions such as Li ions can occupy these sites,[24] as in $Li_4K_6(NbO_3)_{10}$. However, Giess *et al.*[22(a)] immediately appreciated that these materials are really solid solutions and not compounds. Phase-diagram work showed that indeed this was true.[25] Thus, in $A_2B_4Nb_{10}O_{30}$ the ratio of A to B should be variable, for example $A_{2-2x}B_{4+x}Nb_{10}O_{30}$. In this formula, for $x=0.5$, there could be 4.5 Sr^{2+} ions per unit cell and one K^+ ion. Clearly some of the Sr^{2+} ions would have to be on the α sites and most likely in a random manner. Also, $Li_4K_6(NbO_3)_{10}$ could not actually have ten positive ions filling the α, β, and γ sites.[26]

In practice, as we shall see, the situation is complicated. However, the temperature dependence of the dielectric constant is usually a good indication of deviations from some sort of an ordered arrangement to a less-ordered arrangement. Materials with a less-ordered unit cell show broader ϵ-vs-temperature behavior then those with a more-ordered unit cell. This has been observed in many systems.[26-28] Figure 2 presents some data from Ainger *et al.*[27] showing this effect. The sample marked 55 is the closest to the "filled" composition $K_2Sr_4Nb_{10}O_{30}$. The sample marked 88 is the farthest from this composition. As can be seen, the results for sample 88 show a much broader dielectric peak than sample 55.

We have measured the temperature dependence of the index of refraction of two samples whose

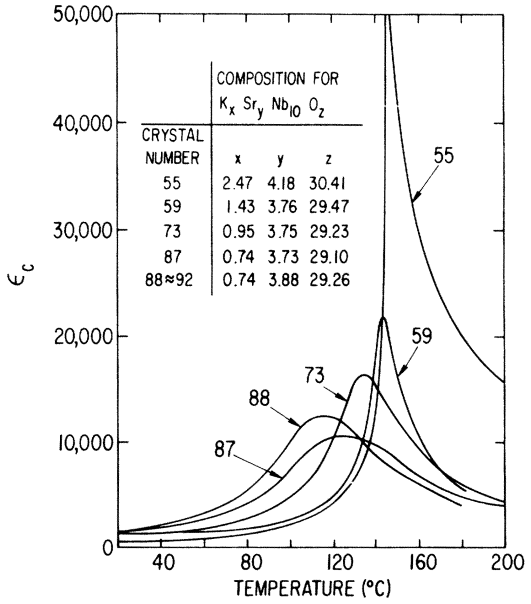

FIG. 2. Temperature dependence of the dielectric constant along the ferroelectric c axis for several different crystal compositions. These data are from Ainger *et al.*, Ref. 27.

numbers are 59 or KSN 59 and 94 or KSN 94. These were grown by Ainger *et al.*[27] The composition and dielectric constant of KSN 59 are shown in Fig. 2. The composition of KSN 94 is the same as KSN 88 shown in Fig. 2. The compositions shown in Fig. 2 are obtained from the chemical-analysis results,[27] which are presented in terms of mole % of K_2O, SrO, and Nb_2O_5. Our temperature-dependent dielectric results are in agreement with those in Fig. 2 except for slight shifts in the peak positions (T_c). These slight shifts of several degrees are undoubtedly due to composition variations between the samples used for Fig. 2 and the samples that we investigated.

Samples of KSN 59 and 94 were prepared into small prisms with an apex angle of approximately 30° for index-of-refraction measurements in the same manner as was done previously.[12] The index of refraction was measured by minimum-deviation techniques using a 6328-Å He-Ne laser in a small temperature-controlled oven.[29]

III. RESULTS

Figure 3 shows the experimental results for the index of refraction for light polarized along the c axis, n_c. This is the ferroelectric axis for these crystals. The arrows in these figures denote the temperature of the peak in the ϵ_c-vs-temperature measurement for the actual prism. For the prism labeled 59, these results were taken as the temperature of the sample was increased. As we shall see, there is an expected thermal hysteresis at T_c in this sample. For the sample labeled 92 the heating and cooling measurements are superimposed and indicate no thermal hysteresis.

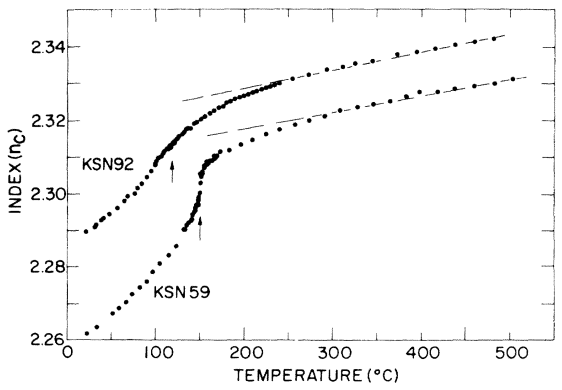

FIG. 3. Temperature dependence of the optic index of refraction for light polarized along the ferroelectric c axis for two $K_2Sr_4(NbO_3)_{10}$-type crystals. The compositions of the crystals are given in Fig. 2. The dashed lines are an extrapolation of the high-temperature data. The arrows indicate the temperatures of the peak of the dielectric constant along the c axis. The measurements are made at 6328 Å.

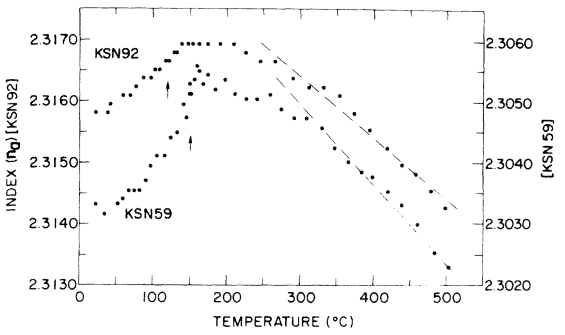

FIG. 4. Temperature dependence of the optic index of refraction for light polarized perpendicular to the ferroelectric axis. The changes in the optic index are much smaller for this axis, and numerical values are given on the left and right for the two different crystals. The dashed line is an attempt to show a high-temperature region. The arrows indicate the temperature of the peak in the dielectric constant along the c axis.

Figure 4 shows the index of refraction n_a for light polarized perpendicular to the c axis (along the a axis) for the same two crystals. The index variation over the entire measured temperature range for n_a is only 0.002 compared to 0.07 for n_c. That the index variation is smaller along the c axis than along the a axis is the usual result for these materials. However, for these samples the anisotropy is much larger than has been observed in most other ferroelectrics with the tungsten-bronze crystal structure. As we shall discuss, the shape of the n_c curve has a qualitative difference

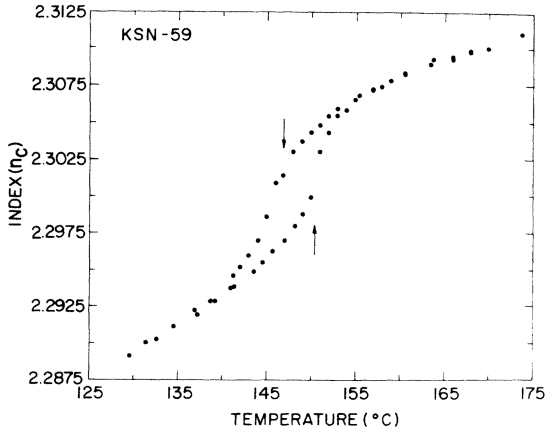

FIG. 5. Results for n_c, as in Fig. 3, but showing the thermal hysteresis for KSN 59 near T_c. The experimental data points as temperature is increased are to the right of the results for decreasing temperature. The arrows show peaks of the dielectric constant along the c axis when the temperature is increased (pointing up) and decreased (pointing down). Thus, the agreement between n_c and ϵ_c is good. See Ref. 30.

from what is expected for ferroelectrics.[2]

Figure 5 shows an expanded plot of n_c vs temperature for the sample KSN 59. A thermal hysteresis is observed between the heating and cooling measurements. The arrows show the positions of the peaks, for heating and cooling of the dielectric constant vs temperature along the c axis. The agreement between the n_c and ϵ_c results is very good. This thermal hysteresis is expected since the crystal undergoes a first-order phase transition. The first-order nature of the transition has been determined by direct measurements of the sign of the B coefficient in the Devonshire free-energy expansion.[30] The sign of this coefficient indicates whether the transition is first or second order, and the results for $K_2Sr_4Nb_{10}O_{30}$ show that the transition is first order. Undoubtedly, the sharpness of the change in n_c is degraded by the compositional inhomogeneities of the sample within the laser-beam diameter, which is about 1 mm. The maximum hysteresis observed in Fig. 5 is ~4.28 °C, which is slightly larger than the 3 °C we obtain from dielectric measurements.

IV. DISCUSSION

In Sec. IV B we will discuss the unusual behavior of the index of refraction shown in Figs. 3 and 4. Before that, however, we will discuss another kind of unusual behavior which we believe is related. This is the disagreement between the dielectric constant calculated from the Lyddane-Sachs-Teller (LST) relation, Eq. (2), and the measured values of the dielectric constant. Then, in Sec. IV C, we discuss qualitatively a model of the transition which brings Secs. IV A and IV B together.

A. $\epsilon(0)$ effect

As was pointed out in Sec. I, in the ferroelectric phase $\epsilon_{cap}/\epsilon_m > 1$, and the ratio gets larger as T approaches T_c from below. We have defined ϵ_{cap} as the clamped dielectric constant measured by standard capacitance techniques and ϵ_m as the dielectric constant obtained from the mode frequencies via the LST relation. This result,[9] $\epsilon_{cap}/\epsilon_m > 1$, is found in[10] $BaTiO_3$, $LiNbO_3$, $LiTaO_3$, as well as in solid solutions of $Pb_{1-x}La_xTi_{1-x/4}O_3$. There are no examples known to the author of a material in the ferroelectric phase that has $\epsilon_{cap}/\epsilon_m = 1$.

Figure 6 shows the temperature dependence[10] of[31] ϵ_{cap} and[10] ϵ_m for $BaTiO_3$. This is the most complete set of data available, in that polariton-type Raman measurements were reported right up to T_c. However, the measurements in $BaTiO_3$ also show the largest ratio of $\epsilon_{cap}/\epsilon_m$. The disagreement at room temperature between ϵ_{cap} and ϵ_m was noted earlier by Pinczuk *et al.*[32] They also found that the second, not the lowest, transverse mode contributes the largest amount to ϵ_m. The results in Refs. 10 and 11 have extended this work to T_c.

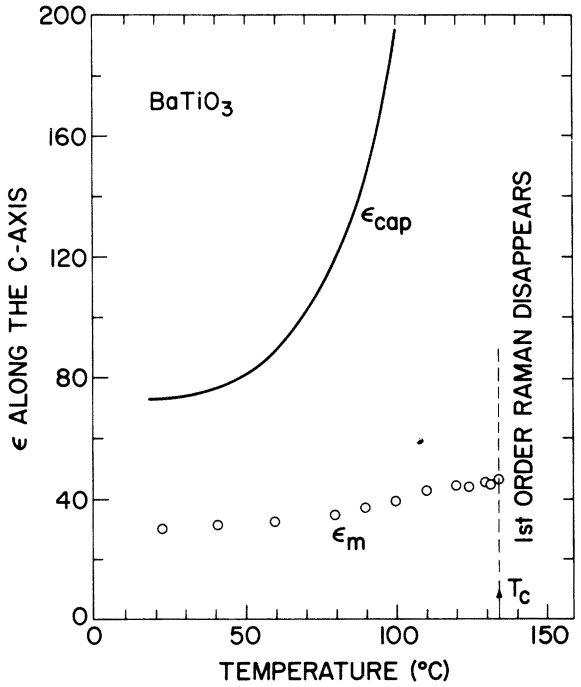

FIG. 6. These results are for $BaTiO_3$. ϵ_m is the result from Eq. (2) using the optic modes measured by polaritons from Ref. 10. ϵ_{cap} is the clamped dielectric constant from Ref. 31. Above T_c the first-order Raman lines abruptly disappear (Ref. 10).

We have shown that it is possible to fit the ϵ_{cap} data by a simple model of a low-frequency localized impurity mode coupled to a higher-frequency mode.[11] This model will be discussed in more detail here. Consider a low-frequency mode, called mode 1, which is coupled to a higher-frequency mode, called mode 2. At present we need not further specify the distinction between the modes, but later we will associate mode 1 with a lattic vibration and mode 2 with the electronic energy levels that determine the optical properties of the material. We will associate these same modes with a localized impurity mode and a low-frequency soft-lattice mode. In either case the formalization is the same, and this is an important point to appreciate. In either case the coupling of the two modes can result in a large enhancement of the dielectric properties. The former case leads to a well-known result, the Szigeti equation. In the latter case, we can explain the $\epsilon_{cap}/\epsilon_m$ results in ferroelectrics.

Writing the usual force-constant equations for these two modes, and using $\omega_i^2 = k_i/m_i$, where ω_i is the bare transverse frequency, k_i is a spring

constant, and m_i is the effective mass of the mode, we have

$$\ddot{x}_1 + \Gamma_1\dot{x}_1 + \omega_1^2 x_1 = (e_1/m_1)E_{\text{loc}} = (e_1/m_1)(E + \gamma_{11}P_1 + \gamma_{12}P_2), \tag{4a}$$

$$\ddot{x}_2 + \Gamma_2\dot{x}_2 + \omega_2^2 x_2 = (e_2/m_2)E_{\text{loc}} = (e_2/m_2)(E + \gamma_{22}P_2 + \gamma_{21}P_1). \tag{4b}$$

The $\Gamma_i\dot{x}_i$ term is a phenomenological velocity-damping term. The field acting on each oscillator is the local field which we have broken up into the external field E and the field produced by the polarization of each mode, where the γ terms are Lorentz factors. In the final results we will set all of these Lorentz factors equal to $\frac{4}{3}\pi$ because of the lack of knowledge of any of the details to pick other Lorentz factors. By taking the time-oscillating form of x, E, $P \sim e^{i\omega t}$ and using

$$P_1 = n_1 e_1 x_1, \quad P_2 = n_2 e_2 x_2, \tag{5}$$

where n_i is the number of oscillators per cm^3, one may solve Eq. (4b) for x_2 in terms of x_1 and E and substitute into Eq. (4a) to obtain Eq. (6a), or one may solve Eq. (4a) for x_1 in terms of x_2 and E and substitute into Eq. (4b) to obtain Eq. (6b):

$$x_1 = \frac{e_1/m_1 + e_2\Delta_2/m_2D_2}{D_1 - \Delta_1\Delta_2/D_2}E, \tag{6a}$$

$$x_2 = \frac{e_2/m_2 + e_1\Delta_1/m_1D_1}{D_2 - \Delta_1\Delta_2/D_1}E, \tag{6b}$$

where the terms in the resonant denominators, D_i and Δ_i, are

$$D_1 \equiv \omega_1^2 - (n_1e_1^2/m_1)\gamma_{11} - \omega^2 + i\omega\Gamma_1,$$

$$D_2 \equiv \omega_2^2 - (n_2e_2^2/m_2)\gamma_{22} - \omega^2 + i\omega\Gamma_2, \tag{7}$$

$$\Delta_1 \equiv (n_1e_1e_2/m_2)\gamma_{21}, \quad \Delta_2 \equiv (n_2e_1e_2/m_1)\gamma_{12}.$$

We may define a susceptibility from the total polarization which is made up of $P_1 + P_2$:

$$P_{\text{total}} = \chi(\omega)E = \{[\epsilon(\omega) - 1]/4\pi\}E = P_1 + P_2 = n_1e_1x_1 + n_2e_2x_2. \tag{8}$$

To obtain a convenient form, we solve Eq. (8) for $\epsilon(\omega)$ by substituting x_2 in terms of x_1 and E, then substituting x_1 in terms of E from Eq. (6a). The result is

$$\epsilon(\omega) - 1 = \frac{(4\pi n_1e_1^2/m_1)[1 + (n_2e_2^2/m_2D_2)\gamma_{12}]^2}{D_1 - \Delta_1\Delta_2/D_2} + \frac{4\pi n_2e_2^2}{m_2D_2}, \tag{9}$$

where we have set $\gamma_{12} = \gamma_{21}$ in the square brackets. This result is general, convenient, and is symmetric in the interchange of oscillators 1 and 2, although this is not instantly apparent at first glance. Equation (9) can be put in a more familiar form by taking a Lorentz factor of $\frac{4}{3}\pi$ and defining

$$\Omega_1^2 \equiv 4\pi n_1e_1^2/m_1, \quad \Omega_2^2 \equiv 4\pi n_2e_2^2/m_2, \quad \gamma_{12} = \tfrac{4}{3}\pi. \tag{10}$$

Then Eq. (9) becomes

$$\epsilon(\omega) = 1 + \frac{\Omega_1^2(1 + \Omega_2^2/3D_2)^2}{D_1 - \Omega_1^2\Omega_2^2/9D_2} + \frac{\Omega_2^2}{D_2}. \tag{11}$$

As an example of this familiar form, we may find the electronic contribution to $\epsilon(\omega)$ by eliminating mode 1, by $e_1 = 0$, and associating oscillator 2 with electronic motion. Then

$$\epsilon_2 \equiv \epsilon_\infty = 1 + \Omega_2^2/D_2 = 1 + \frac{4\pi n_2e_2^2/m_2}{\omega_{T2}^2 - \omega^2 + i\omega\Gamma_2}, \tag{12a}$$

$$\omega_{T2}^2 \equiv \omega_2^2 - 4\pi n_2e_2^2/3m_2, \tag{12b}$$

where we have used $\gamma_{22} = \frac{4}{3}\pi$ in Eq. (12b). Then ω_{T2} is the "dressed" frequency, that is, the observed frequency of resonance as can be seen in Eq. (12a). Equation (12a) is just the familiar form for the frequency dependence of the dielectric constant.

We may also solve Eq. (11) in terms of ϵ_2 in Eq. (11) by noting that from Eq. (12a), $(\epsilon_2 + 2)/3 = 1 + \Omega_2^2/3D_2$. Thus,

$$\epsilon(\omega) = \epsilon_2 + \frac{(4\pi n_1e_1^2/m_1)[(\epsilon_2 + 2)/3]^2}{\omega_1^2 - \frac{1}{3}(4\pi n_1e_1^2/m_1)[(\epsilon_2 + 2)/3] - \omega^2 + i\omega\Gamma_1}. \tag{13}$$

By associating oscillator 2 with the electron system and oscillator 1 with the lattice vibrations we see that this is the Szigeti equation.[33,34] This relation shows that the effect on $\epsilon(\omega)$ is enhanced over what the lattice vibrations by themselves would produce. The enhancement of $(\epsilon_2 + 2)/3$, which is in square brackets, is due to the coupling of the two systems. For the electronic system $\epsilon_2 = \epsilon_{el}$, the square of the index of refraction, is ≈ 2.5 for the alkali halides, so $(\epsilon_{el} + 2)/3$ is not a big enhancement, although for NbO_6 octrahedra materials $(\epsilon_{el} + 2)/3 \approx (2.2^2 + 2)/3 \approx 2.3$ which when squared is a bigger effect. Note that the only assumptions in Eq. (13) are those associated with setting all the Lorentz factors $= \frac{4}{3}\pi$. This means that the atoms or electrons or impurities involved in the mode are localized to a site. For example,

we may not have electrons that are delocalized over several atomic sites or the oscillator in Eq. (4) would just see the external electric field as a driving force and the γP terms would not be appropriate.

We may also interpret the two oscillators in Eqs. (4)–(11) in quite a different manner, which leads to the connection with ferroelectricity. We may take oscillator 2 as the lowest-frequency optic mode of the material and oscillator 1 as an impurity in the lattice that can give rise to a dipole moment with lower frequency than the lowest optic mode. Then the contribution to $\epsilon(\omega)$ and in particular to the clamped dielectric constant $\epsilon(0)$ due to the impurities will be enhanced owing to the coupling of the impurity oscillators to the optic modes just as in Eq. (13). In fact, oscillator 1 will be affected by all the optic modes in the same manner, and the enhancement will be due to all of these modes. In that case we obtain

$$\epsilon(\omega) = \epsilon_\infty + \epsilon_m + \frac{(4\pi n_1 e_1^2/m_1)[(\epsilon_m+2)/3]^2}{\omega_1^2 - \frac{1}{3}(4\pi n_1 e_1^2/m_1)[(\epsilon_m+2)/3] - \omega^2 + i\omega\Gamma_1} \tag{14}$$

Now we can see that the enhancement can be much larger than in the case of the coupling of the electronic oscillator to the ionic modes discussed previously. This is because the optic lattice modes in the tungsten-bronze ferroelectrics give $\epsilon_m \approx 30$, so $(\epsilon_m+2)/3 \approx 10$, which when squared can give sizable effects for a relatively small number of impurities.

To actually attempt to fit[11] ϵ_{cap} in Fig. 6 we divide by $\Omega_1^2 = 4\pi n_1 e_1^2/m_1$ and use the form

$$\epsilon_{cap} = \epsilon_\infty + \epsilon_m + \frac{[(\epsilon_m+2)/3]^2}{p - qT - \frac{1}{3}[(\epsilon_m+2)/3]}, \tag{15}$$

$$p - qT = \omega_1^2/\Omega_1^2.$$

This is just Eq. (14) with $\omega = 0$, since we want to fit the measured value of $\epsilon(0)$ which is called ϵ_{cap}. The reason a temperature factor is put in for ω_1 is that a temperature dependence might be expected even for an impurity in a ferroelectric crystal.

First taking $q = 0$ and using the experimentally measured values of ϵ_m shown in Fig. 6., a value of $p = 6.4$ is found that fits ϵ_{cap}, shown in Fig. 6, very well up to 80 °C. Above 80 °C, however, the experimental ϵ_{cap} increases more rapidly than would be predicted by Eq. (15). Allowing p and q to be nonzero, an excellent fit of ϵ_{cap} can be obtained. The fit is good enough so that deviations are not noticeable in Fig. 6 and thus the fit is not drawn. The values obtained are $p = 13.1$ and $q = 0.200\ K^{-1}$. In the range 20–100 °C, $p - qT$ varies from 7.2 to 5.6, which is a small temperature variation and close to the value required to fit the curve when no temperature dependence is allowed. Two interesting quantities in p are the frequency and density of the impurity, $p \propto \omega_1^2/n_1$. To estimate these quantities we take $\omega_1^2/\Omega_1^2 = 6$. Then we assume that the impurity has the charge of an electron and the mass of a niobium atom. If the resonant frequency ω_1, is 1 cm^{-1}, then $n_1 = 3.4 \times 10^{17}$ cm^{-3} will be needed to explain the data shown in Fig. 6. This is not at all many impurities or deviations from stoichiometry. If we take $\omega_1 = 10$ cm^{-1}, then $n_1 = 3.4 \times 10^{19}$ cm^{-3} is needed, which still is not a very excessive density in these materials. It must be remembered that in the tungsten-bronze ferroelectrics discussed in this paper there are most likely several deviations from the average contents described by the ordered space-group symmetry in every unit cell. Thus, while 10^{19} cm^{-3} may seem like a large number of impurities for $BaTiO_3$, it is not for the tungsten-bronze materials.

For $BaTiO_3$, $\epsilon_{cap}/\epsilon_m > 1$ (≈ 1.5) for the dielectric constants perpendicular to the ferroelectric c axis, but the ratio is closer to 1 than the results shown in Fig. 6, along the c axis.[35] So using the same assumptions about the impurities as above, 10^5 fewer are required to explain the data. Although several possible hypotheses are possible to explain this large anisotropy, we will await experimental evidence for the present.

For $LiNbO_3$ and $LiTaO_3$ the measurements have not been carried as close to T_c as in $BaTiO_3$, so the ratio $\epsilon_{cap}/\epsilon_m$ is temperature dependent but much closer to 1. Thus, very few impurity-type modes would be required to explain the data. Similar to the tungsten-bronze ferroelectrics, these lithium salts are not compounds but really solid solutions over a small range of compositional variation, so several percent of the unit cells can be expected to deviate from the ideal formula unit.

The tungsten-bronze materials have positional disorder[36] besides compositional variation because of the solid solution characteristics. The results for ϵ_m in these materials are a little less clear. A large number of modes have been measured by right-angle Raman scattering[37-41] but, more importantly, by polariton measurements.[42] With the polariton technique, forward Raman scattering, one is much more sure not to miss any modes. The result[42] from the polariton measurements is $\epsilon_m = 30 \pm 5$, independent of temperature! On the other hand, ϵ_{cap} is several orders of magnitude larger near[22] T_c. The problem is that the

polariton measurements were made for $\omega > 30\,\mathrm{cm}^{-1}$. Although modes below 30 cm^{-1} were searched for very carefully[37,42] and not found by right-angle scattering using very small entrance slits on the double monochromator, one cannot absolutely rule out such modes since not every one of the theoretically expected[37,38] modes (18 A_1 modes are expected) have been accounted for. If there are no ordinary optic modes below 30 cm^{-1} then $\epsilon_{\mathrm{cap}}/\epsilon_m$ is indeed large, and the simple and attractive ideas that explain ferroelectricity via the LST relation, Eq. (1), need alteration. This will be discussed below.

B. $\Delta n \propto P^2$ calculation

In this section we show how the data in Figs. 3 and 4 can be interpreted. As will be seen, the result is that a very large part of the crystal is polarized at $T \approx T_c$. This result is, in a certain sense, an extrapolation of the numbers found in Sec. IV A, where $\sim 10^{17}$ cm^{-3} impurities could be contributing to the static dielectric properties in $BaTiO_3$. Here we will argue that a number closer to 10^{23} cm^{-3} are contributing to the square of a polarization above the ferroelectric phase-transition temperature is these tungsten-bronze materials and other dirty displacive ferroelectrics. In Sec. IV C, we show how an extension of the ideas in Sec. IV A can be applied to the problems discussed here.

The basic argument that is used in order to interpret the data shown in Figs. 3 and 4 is related to the quadratic electro-optic effect. This is a very general effect that is allowed in all crystals.[43] For all materials there is a change of the optic index of refraction that is proportional to the square of the polarization. In tensor form this can be written as

$$\Delta(1/n^2)_{ij} = g_{ijkl} P_k P_l, \tag{16}$$

where n is the optic index of refraction, g is the fourth-rank quadratic electro-optic tensor, and P is the polarization. The subscripts run from 1 to 3 for the x, y and z directions. There is a considerable body of literature associated with this equation for the ferroelectric tungsten-bronze materials.[44,45]

Consider the polarization in the high-temperature centrosymmetric phase in Eq. (16) to be made up of a large P_s and a small P_m part, $P = P_s + P_m$. Normally one relates P_s to a ferroelectric spontaneous reversible polarization. P_m is taken as small and can be related to an external applied electric field by the usual small-signal dielectric constant. For the tungsten-bronze ferroelectrics the z or 3 axis is the ferroelectric axis. Specializing Eq. (16) for this case, $\epsilon_3 \gg 1$, $P_m = (\epsilon_3/4\pi)E_3$ in both the high- and low-temperature phase and, using the usual contracted index notation,[43] we obtain

$$\Delta(1/n_2)_j = g_{j3} P_s^2 + (g_{j3} P_s \epsilon_3/2\pi) E_3. \tag{17}$$

The usual ferroelectric interpretation of this equation is that a large spontaneous polarization P_s will cause a centrosymmetric crystal to be biased so that about the bias point there will be a term linear for small fields, E_3 (or small polarization P_m). The second term on the right-hand side of Eq. (17) is just the linear electro-optic effect. It is usually written as rE, where r is the linear electro-optic coefficient, $r = gP_s\epsilon_3/2\pi$. One can measure the quadratic electro-optic effect g above T_c and the linear electro-optic coefficient below T_c and compare the two if P_s and ϵ_3 are known.[44,45] For $K_2Sr_4(NbO_3)_{10}$ these quantities compare very favorably, and the simple but general idea of the biasing of the quadratic electro-optic effect, Eq. (16), explaining the linear electro-optic effect, Eq. (17), agrees with experiment and the constant g is found to have very little temperature dependence.[44-46]

One can also expand the left-hand side of Eq. (16) owing to an appearance of a polarization P,

$$\Delta n_i = n_i^f - n_i^0 = -(n_i^0)^3 g_{i3} P_3^2/2. \tag{18}$$

This equation says that as a polarization is turned from zero to P the index of refraction will deviate from a value n^0, with zero P, to a value n^f with the final amount of polarization. However, it is most important to realize that Δn is proportional to the *square* of the polarization. For example, if different regions are polarized antiparallel and this polarization cannot be reversed, a deviation of the index of refraction from the unpolarized value n^0 still will be observed, even though no ferroelectric-type reversible spontaneous polarization may be observed. The only assumption that goes into Eq. (18) is the idea that the material can be described as a centrosymmetic crystal with a local polarization bias. This will result in a Δn described by Eq. (18).

We would like to use Eq. (18) in connection with the data in Figs. 3 and 4 to determine an average local polarization. To do this one must determine the reference value of the index n^0 and the quadratic electro-optic coefficient g. For $K_2Sr_4(NbO_3)_{10}$ above T_c, a direct measurement has shown[45] that $g_{33} - (n_1/n_3)^3 g_{13} = 0.10$ $\mathrm{m}^4/\mathrm{C}^2$. From the comparison of the experimental values of Δn_3 to Δn_1 using Eq. (18), it was concluded that in the related material $Na_2Ba_4(NbO_3)_{10}$, $g_{33}/g_{13} \approx 3$. However, from Fig. 4 it is clear that Δn_1 is very small, so in the analysis here for $K_2Sr_4(NbO_3)_{10}$-type materials we

conclude that $g_{33}/g_{13} > 10$; we ignore the contribution from g_{13} and therefore we take $g_{33} = 0.10$ m^4/C^2. The determination of n_3^0 over a wide temperature range is perhaps more difficult to do with accuracy. We have taken the high-temperature extrapolation shown in Fig. 3 by the dashed line. In some of our earlier work on $n(T)$ we have taken measurements more than 600 °C above T_c to determine that a linear region for $n(T)$ does indeed exist.[12] From this earlier work[12] and the results shown in Fig. 3, it seems clear that a linear region does exist. However, much below T_c it appears[46] that $n(T)$ really must decrease in slope owing to higher-order terms in Eqs. (16) and (18) becoming important, since far below T_c it would appear that $n_i^f - n_i^0$ increases more slowly than P^2.

Using the extrapolation shown in Fig. 3 and the value of g mentioned in the above paragraph, we determine a value of polarization using Eq. (18). This result for both samples is shown in Fig. 7 as a solid line. As can be seen for the more disordered sample KSN 92, the polarization, or more accurately $|P|$ at T_c, is more than half of its room-temperature value. In the more-ordered sample KSN 59, the result is less than half but still very substantial. The dashed curves in Fig. 7 are a plot of the ferroelectric reversible spontaneous polarization measured by Clarke with a standard Sawyer-Tower hysteresis-loop circuit.[28,47] Below T_c the agreement is quite remarkable, considering there are no adjustable parameters in the solid curve $|P|$ which is obtained from Eq. (18). It is probable that a better value of n^0 below T_c, as discussed in the above paragraph, would put the solid and dashed curves in better agreement, since it would pull the solid curve up at temperatures near room temperature.

Now we would like to discuss the meaning of these large polarizations up to 150 °C above T_c. As we have mentioned in our discussion of the interpretation of the index-of-refraction data in Figs. 3 and 4, these data are sensitive to the projection along the crystallographic axes of the square of an internal polarization. Thus, these data would be sensitive, for example, to a local polarization due to a missing negative ion that could result in a dipole field radially emanating from the missing charge. Clearly, such a volume of the crystal would not result in a reversible spontaneous polarization. Similarly, these data are sensitive to a dynamic polarization in regions of the crystal. From the interpretation of the data as shown in Fig. 7, particularly for the highly disordered material KSN 92, it appears that more than 50% of the volume of the crystal is already polarized at T_c. However, at T_c, or within a small (10–20 °C) range around T_c, the internal fields are strong enough so that the cooperative aspects of the interaction begin to dominate and there is a net reversible polarization for an external field along the z direction. This static polarization model would seem to indicate that the polarization obtained from Fig. 3 via Eq. (18) should always be larger than the reversible spontaneous polarization since there will always be regions that have a $|P|$ but cannot be made to reverse. Although this is not strictly observed in the room-temperature region as can be seen in Fig. 7, the two results are close, and as discussed above we believe a better extrapolation of n^0 will yield this result. If the polarization above T_c were dynamic, both curves could be in close agreement at low temperatures. However, that $|P|$ and the reversible spontaneous polarization are in reasonable agreement at all is encouraging, since $|P|$ is obtained with no adjustable parameters.

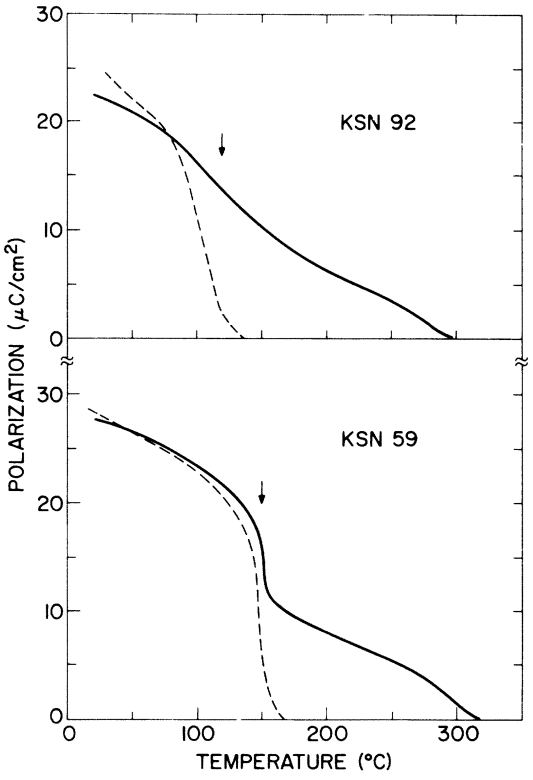

FIG. 7. The solid lines are the square root of the square of the total polarization obtained from Eq. (18) and the data in Fig. 3, as discussed in the text. The dashed lines are the ferroelectric reversible spontaneous polarization measured by Clarke (Ref. 47), and also see Clarke and Burfoot (Ref. 28). There are no adjustable parameters for these curves. The arrows indicate the values of T_c.

C. Qualitative model of the behavior

In materials with as much disorder as KSN 92 it is difficult to talk about optic modes driving the transition in the same way as for normal displacive ferroelectrics.[1] In tungsten-bronze ferroelectric materials, optic modes are observable[37-41] but none could be connected[42] with the dielectric peak of $\epsilon(0)$ as in Eq. (1). In other, very highly disordered perovskite ferroelectric materials we have observed first-order Raman bands,[12] but these bands are more reminiscent of the density of states of the vibrational modes than discrete optic modes.[48] These results are probably similar to the observations in amorphous silicon and germanium where the lack of long-range order breaks the $\vec{k}$ selection rule, and the Raman and infrared observations give a weighted measure of the density of vibrational states.[49]

Thus, in highly disordered materials such as KSN 92, it is unlikely that an optic mode drives the transition at T_c in the conventional manner.[1,2] At T_c more than half the lattice already is polarized, as discussed above. On the other hand, the reason that the lattice can polarize so easily is undoubtedly associated with the close cancellation of the long- and short-range forces,[1,2] and local impurities or disorder weight some regions so that a local polarization, static or dynamic, can occur. As the temperature is lowered thermal vibration decreases, which decreases the volume of the unit cell, which increases the long-range electrostatic forces, which increases the dielectric forces, which increases the dielectric constant, which can allow the polarized volume to increase. Since the material is a ferroelectric, as the temperature is lowered undoubtedly the volume that will eventually favor a reversible polarization with a projection along the z axis grows. At T_c, since there is no break in the $n(T)$ curve in very disordered materials as can be seen for KSN 92 and some of the earlier results,[12] there is no discontinuous change in the amount of volume of the crystal that is polarized. However, comparing KSN 92 to KSN 59, one may see how this varies with the disorder in the crystal. One can imagine how, as the crystals become more highly ordered, a polarization as measured by $n(T)$ will only occur below T_c. This is, of course, the expected classical behavior.[1,2]

We would like to describe a mechanism that will cause the low-frequency dielectric constant to increase a great deal and which will drive the transition leading to the observations shown in Fig. 7. With reference to Eq. (14), consider that at least some of the disorder can be treated as localized centers that are coupled to optic modes as described in Sec. IV A. Those localized centers with the highest oscillation frequency we call f, those with lower oscillation frequency we call g, and those with still lower oscillation frequency we call h, etc. By applying the coupled equations discussed previously we find that the dielectric constant due to the f oscillators can be described by Eq. (14) where the subscript f should replace the subscript 1, and ϵ_m is the effect caused by all the optic modes. This has been discussed in Sec. IV A. Then the dielectric constant due to the g oscillators can be described by Eq. (14). Now the subscript g should replace the subscript 1 in this equation, while ϵ_m now refers to the dielectric constant due to optic modes plus the effect of f oscillators which have already been enhanced. This process continues for the h oscillators, etc. Thus, we may see how this enhancement can be very effective in causing very large dielectric constants. Clearly, this process must be described by a distribution of oscillators with a distribution of frequencies. However, lack of experimental knowledge for the low-frequency (0.5–30 cm^{-1}) range in these materials makes quantitative estimates impossible at this time, although there is some understanding of the frequency-dependent dielectric constant in the tungsten-bronze materials.[50,51] The difference between dirty displacive ferroelectrics and materials like $BaTiO_3$ is interesting to note. For $BaTiO_3$, we noted in Sec. IV A that 10^{17} to 10^{19} cm^{-3} impurities are needed to explain the zero frequency-clamped dielectric constant. However, for the tungsten-bronze ferroelectrics, as best as we can tell, the optic modes have no temperature dependence in the ferroelectric phase. Thus, impurities of a much larger concentration are needed to account for $\epsilon(0)$. Indeed, they exist in these materials since every unit cell has built-in disorder. Thus, there are essentially 10^{23} cm^{-3} impurities, and it is clear that the application of these ideas can cause very large dielectric constants.

Then, resulting from the effects described above, some regions in the crystal can have very large dielectric constants, causing a local polarization which would be observed as an index change because of the effects discussed in Sec. IV B. Again we see how essentially the entire crystal (all of the unit cells) must be involved, since the polarization results shown in Fig. 7 for KSN 92 indicate that at least half of the crystal is polarized just above T_c.

D. Related comments

There have been several reports of broad, low-frequency, structureless Raman scattering[41,52,53]

in the tungsten-bronze ferroelectrics. Actually, this increase in intensity as T_c is approached from below was found in the early Raman work,[37] although it was not emphasized there. Clarke and Siapkas[52,53] have fitted the temperature dependence of this broad response to a Debye function. They also present some measurements of the dielectric constant at room temperature and at 10 cm^{-1} that indicate that there indeed may be a broad relaxation of $\epsilon(\omega)$ in these materials. The broad structureless Raman scattering can also be seen above T_c. It is possible that these observations are consistent with the model proposed here, i.e., that localized polarized regions allow first-order Raman scattering but the regions are sufficiently nonuniform or last for a sufficiently short time that only a broad structureless response is observed.[54-56] It should be noted that, for the materials discussed here, $\approx$150 °C ($\approx$100 cm^{-1}) is a characteristic temperature. For example, Fig. 3 shows deviations from the expected behavior in ferroelectrics starting at $T_c + 150$ °C. The energy corresponding to this temperature is of the order of magnitude of the broad Raman response. Smolenskii *et al.*[57] have also reported some scattering measurements that might be consistent with the model proposed here.

The ideas discussed in Sec. IV C may also be relevant to the much-discussed[54-56] broad Raman structure observed in $BaTiO_3$. However, we hasten to add that in $BaTiO_3$ there are $3n-3$ optic modes that indeed behave properly,[32] and disappear abruptly[10,35] at T_c. One should not confuse the $3n-3$ optic modes with the broad Raman response.

It is also possible that the ideas discussed here might be related to the "central peak" that has been observed[58] and extensively discussed.[59] The local disorder, static and possibly dynamic, would provide alternate paths for relaxation which could lead to a central peak. The equations developed here will give a peak in $\epsilon(\omega)$ at $\omega \approx 0$ for any overdamped mode. For example, if $\Gamma_1/\omega_1 \gg 0$ in Eq. (13), then $\epsilon(\omega)$ will have a very intense peak at $\omega \approx 0 \ll \omega_1$.

ACKNOWLEDGMENTS

The crystals used for the optic-index measurements were very generously supplied by Dr. R. Clarke. I am indeed grateful for this loan. Very helpful discussions have taken place between myself and E. Burstein, R. Clarke, E. Pytte, N. Shiren, and B. D. Silverman. The technical assistance of F. Dacol is very much appreciated.

---

*A preliminary account of this work appeared in G. Burns and R. Clarke, Bull. Am. Phys. Soc. 19, 279 (1974).

†Partially supported by the Army Research Office, Durham, N. C.

[1]W. Cochran, Phys. Rev. Lett. 3, 412 (1959); Adv. Phys. 9, 387 (1960); 10, 401 (1961).

[2](a) F. Jona and G. Shirane, *Ferroelectric Crystals* (Macmillan, New York, 1962); (b) E. Fattuzzo and W. J. Merz, *Ferroelectricity* (Wiley, New York, 1967); (c) W. Kaenzig, in *Solid State Physics*, edited by F. Seitz and D. Trunbull (Academic, New York, 1957), Vol. 4, pp. 1–197.

[3]A. S. Barker, Jr. and M. Tinkham, Phys. Rev. 125, 1527 (1962).

[4]R. A. Cowley, Phys. Rev. Lett. 9, 159 (1962); Phys. Rev. 134, A981 (1964).

[5]C. H. Perry and T. F. McNelly, Phys. Rev. 154, 456 (1967).

[6]G. Shirane, R. Nathans, and V. J. Minkiewicz, Phys. Rev. 157, 396 (1967).

[7]W. G. Spitzer, R. C. Miller, D. A. Kleinman, and L. E. Howarth, Phys. Rev. 126, 1710 (1962).

[8]T. M. Ballantyne, Phys. Rev. 136, A429 (1964); A. S. Barker, Jr., Phys. Rev. 145, 931 (1966).

[9]G. Burns and B. A. Scott, Solid State Commun. 13, 417 (1973); see also G. Burns and B. A. Scott, Bull. Am. Phys. Soc. 18, 476 (1973).

[10]G. Burns, Phys. Lett. A 43, 271 (1973).

[11]G. Burns and E. Burstein, Ferroelectrics 7, 297 (1974). (This work was presented at the International Ferroelectrics Conference, Edinburgh, in September, 1973.)

[12]G. Burns and B. A. Scott, Solid State Commun. 13, 423 (1973).

[13]F. S. Glasso, *Structure, Properties and Preparation of Perovskite Type Compounds* (Pergamon, New York, 1969).

[14]G. A. Smolensky, J. Phys. Soc. Jpn. Suppl. 28, 26 (1970). This work summarizes a great deal of work and references can be found in it to the original papers.

[15]R. M. Hill and S. K. Ichiki, Phys. Rev. 128, 1140 (1962); 130, 150 (1963).

[16]I. Hatta, J. Phys. Soc. Jpn. 24, 1043 (1968); also, see references to the earlier work quoted there.

[17]E. V. Chisler and M. S. Shun, Phys. Status Solidi 17, 173 (1966).

[18]P. da R. Andrade, A. D. Prasad Rao, R. S. Katiyan, and S. P. S. Porto, Solid State Commun. 12, 847 (1973).

[19]H. Vogt and H. Happ, Phys. Status Solidi 16, 711 (1966).

[20]J. D. Axe, Phys. Rev. 167, 573 (1968).

[21]M. H. Francombe and B. Lewis, Acta Cryst. 11, 696 (1958).

[22](a) E. A. Giess, G. Burns, D. F. O'Kane, and A. W. Smith, Appl. Phys. Lett. 11, 233 (1967); (b) G. Burns, E. A. Giess, D. F. O'Kane, and B. A. Scott, Bull. Am. Phys. Soc. 112, 1078 (1967); (c) D. F. O'Kane, E. A. Giess, G. Burns, and B. A. Scott, *ibid.*, 112, 1079 (1967).

[23]J. E. Geusic, H. J. Levinstein, J. J. Rubin, S. Singh, and L. S. Van Uitert, Appl. Phys. Lett. 11, 269 (1967).
[24]L. G. Van Uitert, S. Singh, H. J. Levinstein, J. E. Geusic, and W. A. Bonner, Appl. Phys. Lett. 11, 161 (1967).
[25]B. A. Scott, E. A. Giess, and D. F. O'Kane, Mater. Res. Bull. 4, 107 (1969).
[26]B. A. Scott, E. A. Geiss, B. L. Olson, G. Bruns, A. W. Smith, and D. F. O'Kane, Mater. Res. Bull. 5, 47 (1970).
[27]F. W. Ainger, J. A. Beswick, S. G. Porter, and R. Clarke, Ferroelectrics 3, 321 (1972).
[28]R. Clarke and J. C. Burfoot, Ferroelectrics 8, 505 (1974).
[29]G. Burns and B. A. Scott, Phys. Rev. B 7, 3088 (1973).
[30]G. Burns, D. F. O'Kane, E. A. Giess, and B. A. Scott, Solid State Commun. 6, 223 (1968).
[31]S. H. Wemple, M. DiDomenico, Jr., and I. Camlibel, J. Phys. Chem. Solids 29, 1797 (1968); also, see I. Camlibel, M. DiDomenico, Jr., and S. H. Wemple, J. Phys. Chem. Solids 31, 1417 (1970).
[32]A. Pinczuk, E. Burstein, and S. Ushioda, Solid State Comm. 7, 139 (1969); A. Pinczuk, Thesis (University, 1969) (unpublished).
[33]B. Szigeti, Trans. Faraday Soc. 45, 155 (1949).
[34]Also see E. Burstein, in *Phonons and Phonon Interactions*, edited by T. A. Bok (Benjamin, New York, 1964), p. 276.
[35]G. Burns, Phys. Rev. B 10, 1951 (1974).
[36]P. B. Jamison, L. C. Abrahams, and J. L. Bernstein, J. Chem. Phys. 48, 5048 (1968); 50, 4352 (1969); 54, 2355 (1971).
[37]G. Burns, J. D. Axe, and D. F. O'Kane, Solid State Commun. 7, 933 (1969).
[38]G. Burns, E. A. Giess, D. F. O'Kane, B. A. Scott, and A. W. Smith, J. Phys. Soc. Jpn. Suppl. 28, 153 (1970).
[39]S. D. Ross, J. Phys. C 3, 1785 (1970).
[40]E. Anzallag, T. S. Chang, R. H. Pantell, and R. S. Feigelson, J. Appl. Phys. 42, 3254 (1971).
[41]L. C. Bobb, J. Dahl, I. Lefkowitz, and L. Muldawar, Ferroelectrics 1, 247 (1970); 2, 217 (1971).
[42]G. Burns, Appl. Phys. Lett. 20, 230 (1972); also see G. Burns, in *Polaritons*, edited by E. Burstein and F. DeMartini (Pergamon, New York, 1974), p. 45.
[43]For example, see J. F. Nye, *Physical Properties of Crystals* (Oxford U. P., Oxford, England, 1957).
[44]For example see G. Burns, IEEE Trans. Electron Devices ED-16, 506 (1969).
[45]G. Burns and A. W. Smith, IEEE J. Quantum Electron. QE-4, 584 (1968).
[46]A. W. Smith, G. Burns, and D. F. O'Kane, J. Appl. Phys. 42, 250 (1971). A. W. Smith, G. Burns, B. A. Scott, and H. D. Edmonds, J. Appl. Phys. 42, 684 (1971).
[47]R. Clarke (private communication).
[48]R. Shaker and R. W. Gammon, Phys. Rev. Lett. 25, 22 (1970).
[49]J. E. Smith, M. H. Brodsky, B. L. Crowder, M. I. Nathan, and A. Pinczuk, Phys. Rev. Lett. 26, 642 (1971).
[50]See, for example, A. M. Glass, J. Appl. Phys. 40, 4699 (1969).
[51]Relaxation in dielectrics is discussed by V. V. Daniel, *Dielectric Relaxation* (Academic, New York, 1967). Chapter 16 discusses some relaxation measurements in ionic ferroelectrics.
[52]D. Siapkas and R. Clarke, Phys. Status Solidi B 62, 43 (1974).
[53]R. Clarke and D. Siapkas, J. Phys. C 8, 377 (1975).
[54]M. DiDomenico, Jr., S. P. S. Porto, and S. H. Wemple, Phys. Rev. Lett. 19, 855 (1967).
[55]M. P. Fontana and M. Lambert, Solid State Commun. 10, 1 (1972); A. M. Quittet and M. Lambert, Solid State Commun. 12, 1053 (1973).
[56]G. A. Barbosa, A. Chaves, and S. P. S. Porto, Solid State Commun. 11, 1053 (1972).
[57]G. A. Smolenskii, V. A. Trepakov, and N. N. Krainik, Zh. Eksp. Teor. Fiz. Pis'ma Red. 20, 322 (1974) [JETP Lett. 20, 143 (1974)].
[58]T. Riste, E. J. Samuelsen, K. Otnes, and J. Feder, Solid State Commun. 9, 1455 (1971).
[59]For example, see E. Pytte, Comments Solid State Phys. 5, 41 (1973); 5, 57 (1973); S. M. Shapiro, J. D. Axe, G. Shirane, and T. Riste, Phys. Rev. B 11, 4332 (1972).